Neuron, Vol. 37, 275–286, January 23, 2003, Copyright ©2003 by Cell Press

Glial Glutamate Transporters Mediate a Functional Metabolic Crosstalk between Neurons and Astrocytes in the Mouse Developing Cortex

Brigitte Voutsinos-Porche,[1,7] Gilles Bonvento,[1,2,7] Kohichi Tanaka,[3] Pascal Steiner,[4] Egbert Welker,[5] Jean-Yves Chatton,[6] Pierre J. Magistretti,[6] and Luc Pellerin[6,*]

[1]CNRS FRE 2363
Paris
[2]CNRS CEA URA2210
Service Hospitalier Frederic Joliot
Orsay
France
[3]Medical Research Institute
Tokyo Medical and Dental University
Tokyo
Japan
[4]Faculté des Sciences de la Vie
Ecole Polytechnique Fédérale de Lausanne
[5]Institut de Biologie Cellulaire
et de Morphologie and
[6]Institut de Physiologie
Université de Lausanne
Lausanne
Switzerland

Summary

Neuron-glia interactions are essential for synaptic function, and glial glutamate (re)uptake plays a key role at glutamatergic synapses. In knockout mice, for either glial glutamate transporters, GLAST or GLT-1, a classical metabolic response to synaptic activation (i.e., enhancement of glucose utilization) is decreased at an early functional stage in the somatosensory barrel cortex following activation of whiskers. Investigation in vitro demonstrates that glial glutamate transport represents a critical step for triggering enhanced glucose utilization, but also lactate release from astrocytes through a mechanism involving changes in intracellular Na^+ concentration. These data suggest that a metabolic crosstalk takes place between neurons and astrocytes in the developing cortex, which would be regulated by synaptic activity and mediated by glial glutamate transporters.

Introduction

Glial cells have long been thought to assume a purely passive role of structural support and maintenance of homeostasis for neurons. Mounting evidence however suggests that they have much more important and dynamic functions. Because of their capacity to detect and respond to neuronal activity, glial cells, and in particular astrocytes, may be an integral part of the communication network within the central nervous system. Among their new emerging roles, glial cells have been shown to enhance synapse number and spontaneous synaptic activity between developing neurons in culture and to play a role in the stabilization and maintenance of synapses (Pfrieger and Barres 1997; Ullian et al., 2001). Moreover, modulation of synaptic transmission by glial cells has been described at the neuromuscular junction (Robitaille, 1998), in hippocampal cultures (Araque et al., 1998), as well as in the retina (Newman and Zahs, 1998). Multiple molecules and signals must therefore be exchanged between glia and neurons to ensure optimal efficiency of the nervous system.

Astrocytes are particularly well suited for interacting with neurons. Each astrocyte contacts several neurons with processes that ensheath synapses (Grosche et al., 1999). Moreover, two of the five subtypes of glutamate transporters identified so far, GLAST and GLT-1, are predominantly located on astrocytes, allowing them to be responsible for most of glutamate uptake (Danbolt, 2001). Indeed, glutamate is predominantly converted to glutamine in astrocytes and returned to neurons in order to replenish the presynaptic neurotransmitter pool and help maintain synaptic transmission (Sibson et al., 2001). Astrocytes also express a number of neurotransmitter receptors, and they specifically respond to synaptic activity via these receptors, as exemplified by the excitatory neurotransmitter glutamate (Gallo and Ghiani, 2000). Although astrocytes do not display major changes of their membrane potential in response to neuronal activation, they do exhibit other forms of excitability. For example, rythmic elevations of intracellular Ca^{2+} levels produced via a glutamate-receptor-dependent mechanism have been described (Kim et al., 1994).

Another classical role attributed to astrocytes has been to ensure an adequate metabolic supply to neurons. One early observation to suggest this function was their particular localization between blood vessels and neurons (Andriezen, 1893). Astrocytes also possess specialized processes called end-feet that come in close contact with capillaries, covering their surface almost entirely (Kacem et al., 1998). In addition, these processes express glucose transporters (Morgello et al., 1995), suggesting that astrocytes may constitute a privileged site of glucose uptake as it penetrates within the brain parenchyma. Up to now, direct evidence for a role of astrocytes in the regulation of energy metabolism has been scarce. A series of results obtained in vitro have led to the hypothesis that synaptic activity at glutamatergic synapses could be detected by astrocytes via glutamate transport activity and would be translated into a metabolic signal (Pellerin and Magistretti, 1994; Poitry-Yamate et al., 1995). The mechanism proposed would provide a means to deliver energy substrates on demand to face energy needs upon increased neuronal activity (Magistretti et al., 1999).

We chose to study a classical metabolic response to synaptic activation, enhancement of glucose utilization, in the mouse somatosensory cortex at postnatal day 10 (P10), a time when this metabolic response was shown to be maximal (Melzer et al., 1994). Here we report that glucose utilization induced by activation of the whisker-to-barrel pathway is decreased in the somatosensory

*Correspondence: luc.pellerin@iphysiol.unil.ch
[7]These authors contributed equally to this work.

cortex of P10 mutant mice for each glial glutamate transporter, GLAST and GLT-1. We also demonstrate, using in vitro preparations from these neonatal mutant mice, that the reduced metabolic response is likely due to a decrease of glutamate transport and intracellular Na^+ signal in cortical astrocytes. Finally we show that astrocytes, following glutamate uptake, release lactate and suggest it could be used as a supplementary energy substrate by neurons during periods of synaptic activity. Our results provide strong evidence supporting the existence of a metabolic crosstalk between astrocytes and neurons that would be mediated by glial glutamate transporters and could be important at least during development for sustaining neuronal functions.

Results

Prominent Expression of GLAST and GLT-1 in the Somatosensory Barrel Cortex of Developing Mice

Expression of glial glutamate transporters GLAST and GLT-1 was determined in the somatosensory barrel cortex of *GLAST*$^{+/+}$, *GLAST*$^{-/-}$, *GLT-1*$^{+/+}$, and *GLT-1*$^{-/-}$ mice for each transporter at an early stage of functional development (postnatal day 10). Immunolabeling of GLAST and GLT-1 performed on tangential sections through layer IV of the primary somatosensory cortex of P10 *GLAST* or *GLT-1*$^{+/+}$ mice revealed the entire vibrissae-related pattern (Figures 1A and 1E, respectively). Therefore, at this age, barrels forming all major five rows are enriched in both glial glutamate transporters. The immunoreactivity was confined to the barrels, leaving septa relatively free of staining (Figures 1B and 1F). In *GLAST*$^{-/-}$ (Figure 1C) and *GLT-1*$^{-/-}$ (Figure 1G) mice, immunoreactivity for the corresponding transporter was completely absent. No obvious upregulation of the other nontargeted glial glutamate transporter was observed in both cases (Figures 1D and 1H). Nissl and cytochrome oxidase stainings performed on sections from both P10 *GLAST*$^{-/-}$ and *GLT-1*$^{-/-}$ mice revealed a normal patterning in the somatosensory barrel cortex and a complete segregation of the thalamocortical afferents (data not shown).

Unaltered Expression of Other Synaptic and Glial Components of the Glutamatergic System in the Cortex of *GLAST*$^{-/-}$ and *GLT-1*$^{-/-}$ Mice

The relative level of expression of the glial glutamate transporters GLAST and GLT-1, the neuronal glutamate transporter EAAC1, the key glial enzyme for glutamate recycling glutamine synthetase (GS), and two different subtypes of glutamatergic postsynaptic receptors, GluR1 and NR2A/B, was measured by immunoblotting in cortical fractions from corresponding *GLAST*$^{+/+}$, *GLAST*$^{-/-}$, *GLT-1*$^{+/+}$, and *GLT-1*$^{-/-}$ mice (n = 3 for each) (Figure 2). Glutamate transporter antibodies detected distinct proteins in cortex homogenates with molecular weights of ~65, 72, and 69 kDa for GLAST, GLT-1, and EAAC1, respectively. Apparent homomultimers (mainly dimers) of GLAST, GLT-1, and EAAC1 were observed as previously shown (Haugeto et al., 1996). To ensure that protein levels were comparable under each condition, each blot was probed for actin. The absence of immunoreactive bands for either GLAST or GLT-1 confirmed the phenotype of *GLAST*$^{-/-}$ and *GLT-1*$^{-/-}$ mice, respectively. Semiquantitative evaluation of the relative level of expression of the three glutamate transporters confirmed the absence of overexpression of the other nontargeted glutamate transporters in each case. No significant change in the expression of glutamine synthetase, GluR1, and NR2A/B was noted in *GLAST*$^{-/-}$ and *GLT-1*$^{-/-}$ mice as compared to their respective *GLAST*$^{+/+}$ and *GLT-1*$^{+/+}$ control.

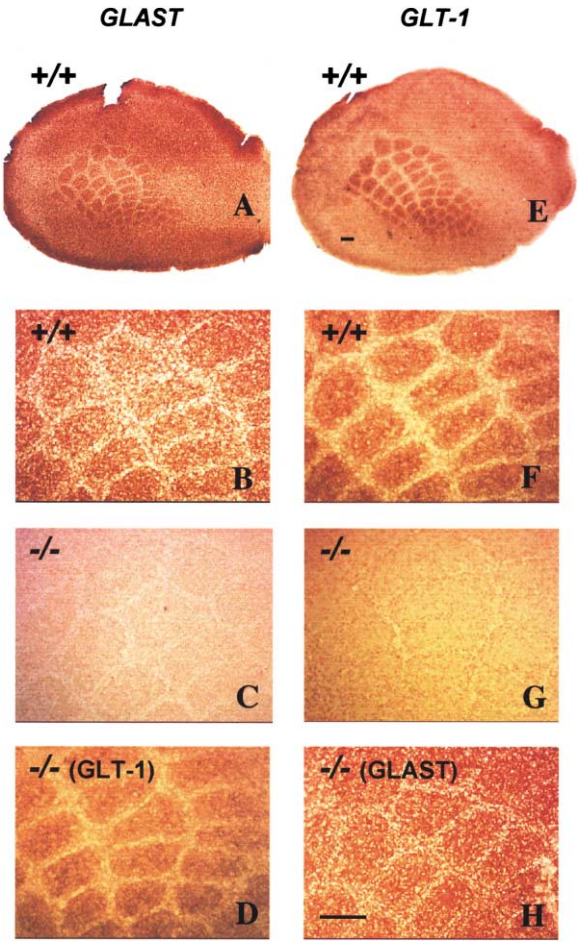

Figure 1. GLAST and GLT-1 Immunohistochemical Staining in the Barrel Cortex of Normal as Well as *GLAST* and *GLT-1* Mutant Mice at P10

(A–H) Sections of P10 *GLAST*$^{+/+}$ (A and B), *GLT-1*$^{+/+}$ (E and F), *GLAST*$^{-/-}$ (C and D), and *GLT-1*$^{-/-}$ (G and H) mice were cut tangentially through layer IV of the right somatosensory cortex. GLAST (A and B) and GLT-1 (E and F) immunoreactivity on sections from *GLAST*$^{+/+}$ and *GLT-1*$^{+/+}$ mice showed individual cell clusters corresponding to mystacial vibrissae. Immunoreactivity for GLAST (C) or GLT-1 (G) was completely absent in the respective *GLAST*$^{-/-}$ and *GLT-1*$^{-/-}$ mice. No apparent upregulation of expression of either GLT-1 in *GLAST*$^{-/-}$ mice (D) or of GLAST in *GLT-1*$^{-/-}$ mice (H) was observed. Scale bar, 200 μm.

Reduced Metabolic Response to Whisker Stimulation in Somatosensory Cortex of P10 *GLAST* and *GLT-1* Mutant Mice

Accumulation of 2-deoxyglucose (2-DG) is used classically to determine the level of neuronal activation in

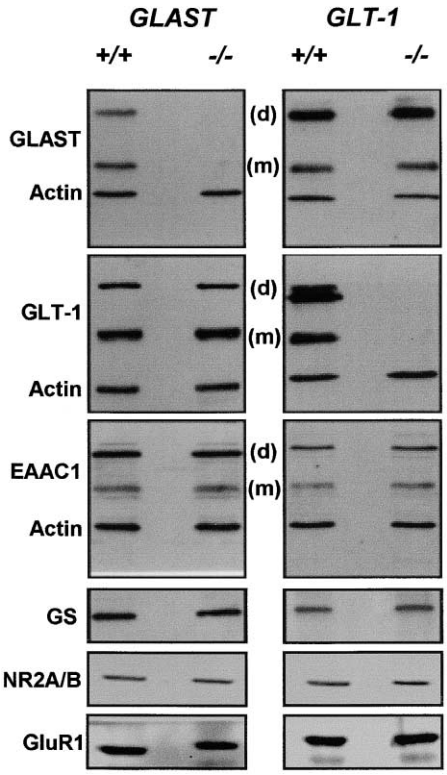

Figure 2. Expression of Different Glial and Neuronal Components of the Glutamatergic System in the Cortex of Normal as Well as *GLAST* and *GLT-1* Mutant Mice at P10

Immunoblots confirmed the absence of GLAST and GLT-1 in the respective *GLAST*$^{-/-}$ and *GLT-1*$^{-/-}$ mice. The relative expression of GLAST or GLT-1, EAAC1, glutamine synthetase (GS), NR2A/B, and GLUR1 was unchanged in *GLAST*$^{-/-}$ and *GLT-1*$^{-/-}$ mice compared to *GLAST*$^{+/+}$ and *GLT-1*$^{+/+}$ animals. GLAST, GLT-1, and EAAC1 displayed both monomer (m) and dimer (d) bands.

specific brain areas. This method has been used successfully in several paradigms including activation of a somatosensory pathway such as the whisker-to-barrel system. To explore the possible implication of glial glutamate transporters in the regulation of this functional metabolic response, mutant animals for either *GLAST* or *GLT-1* were used. For all experiments, P10 *GLAST*$^{+/+}$ and *GLAST*$^{-/-}$ or *GLT-1*$^{+/+}$ and *GLT-1*$^{-/-}$ littermates were comparatively examined. In *GLAST*$^{+/+}$ or *GLT-1*$^{+/+}$ mice, stimulation of the two caudalmost follicles of row C (C1C2) evoked an increase in 2-DG uptake in the corresponding barrels of somatosensory cortex as seen in both coronal (Figures 3A and 3E) and tangential sections (Figures 3C and 3G). The activated zone was observed in four to six consecutive sections. The level of 2-DG uptake in C1C2 barrels measured on tangential sections was 16.8% $\pm$ 4.9% ($n = 8$ for *GLAST*) and 15.6% $\pm$ 5.0% ($n = 8$ for *GLT-1*) above the level measured in the unstimulated barrels of the reference area. In *GLAST*$^{-/-}$ mice, 2-DG uptake induced by repetitive stimulation of the C1C2 whiskers was significantly lower (5.3% $\pm$ 4.9%; -68%, $p < 0.05$, $n = 4$) (Figures 3B and 3D). In parallel, *GLT-1*$^{-/-}$ animals also exhibited a significantly lower 2-DG uptake (6.3% $\pm$ 5.6%; -60%, $p < 0.05$, $n = 11$) (Figures 3F and 3H). In order to ensure that this effect was not the consequence of an increase in excitability in these mutant animals that would occlude any evoked metabolic response, we compared basal 2-DG uptake measured in adjacent nonactivated barrels between *GLAST*$^{+/+}$ and *GLAST*$^{-/-}$ or *GLT-1*$^{+/+}$ and *GLT-1*$^{-/-}$ mice. No significant difference was found in basal 2-DG uptake between *GLAST*$^{+/+}$ and *GLAST*$^{-/-}$ animals (136 $\pm$ 26 versus 135 $\pm$ 4 nCi/g, respectively; $p = 0.922$, Student's t test), nor between *GLT-1*$^{+/+}$ and *GLT-1*$^{-/-}$ mice (227 $\pm$ 84 versus 242 $\pm$ 35 nCi/g, respectively; $p = 0.466$, Student's t test). The difference in basal uptake between *GLAST*$^{+/+}$ and *GLT-1*$^{+/+}$ mice is most likely due to background strain differences. Additional pharmacological experiments were performed to tentatively assess the contribution of glutamate receptor activation to the metabolic response. For this purpose, P10 C57 BL/6 mice were injected with either an NMDA antagonist (MK-801, 0.05 mg/kg, $n = 5$) or an AMPA/KA antagonist (NBQX, 20 mg/kg, $n = 6$) 10 min before 2-DG administration, while three mice served as control. No significant decrease in 2-DG uptake measured in C1C2 was observed after blockade of AMPA/KA receptors (19.3% $\pm$ 2.5% versus 23.7% $\pm$ 3.8% in control mice), or after injection of the NMDA receptor antagonist MK-801 in which case it was even significantly increased (35.7% $\pm$ 10.3%, ANOVA plus Dunnett's test, $p < 0.05$).

Reduction of Glutamate Uptake in Primary Cultures of Cortical Astrocytes from Neonatal Mutant Mice Prevents the Enhancement in Aerobic Glycolysis Triggered by Glutamate

In order to understand how the absence of a glial glutamate transporter could affect the normal functional metabolic response in vivo as measured with the 2-deoxyglucose accumulation method, we turned to primary cultures of cortical astrocytes from these neonatal transgenic mice. Immunoblotting experiments showed that GLAST was strongly expressed in all cultures except in those from *GLAST*$^{-/-}$ mice where it was absent (Figure 4A). In contrast, signal for GLT-1 remained below detection levels in all cases with the revelation technique used (data not shown). These results are consistent with previous studies showing a predominant expression of GLAST in primary cultures of cortical astrocytes from neonatal mice (Stanimirovic et al., 1999). Since we also determined that GLT-1 does not participate to overall glutamate uptake in neonatal cultured astrocytes (data not shown), we took advantage of this simplified situation to evaluate the impact of the selective reduction of GLAST expression in astrocytes from *GLAST* mutant mice on both glutamate uptake and the metabolic response of these cells to glutamate exposure. First, immunohistochemical labelings were performed with antibodies directed against GLAST and the astroglial marker glial fibrillary acidic protein (GFAP) in order to characterize the phenotype of cultured cells. Astrocytes from *GLAST*$^{+/+}$ and *GLAST*$^{+/-}$ mice exhibited immunoreactivity for GLAST while none could be detected in cultured cells from *GLAST*$^{-/-}$ mice (Figure 4B). We also ascertained that >95% of cells were GFAP positive and no MAP2-positive cell was detected (data not shown). Then, glutamate uptake capacity was evaluated in cortical astrocytes cultures prepared from each type of neo-

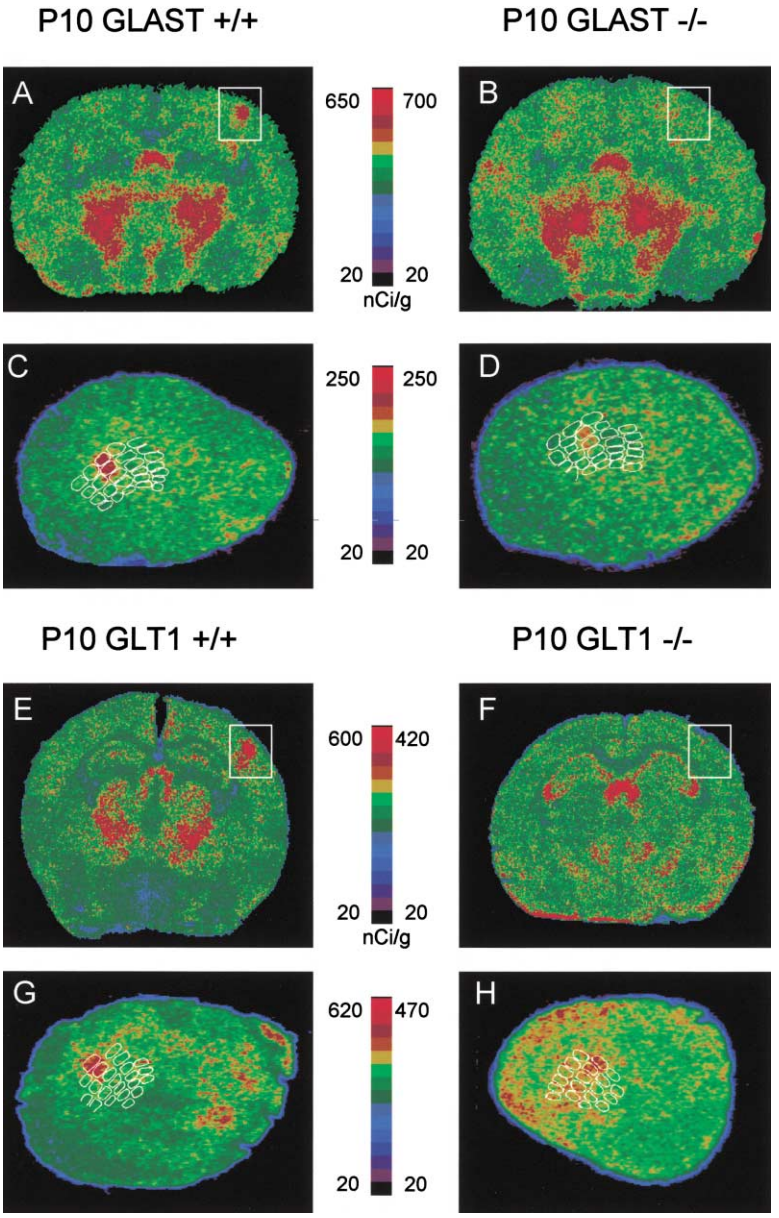

Figure 3. Effect of Unilateral C1C2 Whisker Stimulation on 2-DG Uptake in Somatosensory Cortex of P10 *GLAST* and *GLT-1* Mutant Mice

(A–H) Representative pseudocolored digitized autoradiograms were obtained either from antero-posterior coronal sections at the level of the somatosensory barrel field or from tangential sections through layer IV of the primary somatosensory cortex. The level of 2-DG uptake is color coded according to the respective colored scales. Unilateral left or bilateral C1C2 whisker stimulation in *GLAST*$^{+/+}$ and *GLT-1*$^{+/+}$ mice produced a local increase in 2-DG uptake in the right somatosensory cortex (white square, [A] and [E]) that was restricted to the C1C2 barrels (C and G). In *GLAST*$^{-/-}$ and *GLT-1*$^{-/-}$ mice, increase in 2-DG uptake was not detectable in coronal sections (white square, [B] and [F]) while a faint metabolic response could be identified and quantitated in the C1C2 barrels when the brain was cut tangentially to the barrel field (D and H).

natal *GLAST* mutant mice. This was performed using as substrate D-aspartate, a nonmetabolizable glutamate analog, at two distinct concentrations which correspond to a value close to previously reported K_m (50 μM) or sufficient to approach V_{max} (500 μM) in cortical astrocytes (Debernardi et al., 1999). A reduction of D-aspartate uptake at both 50 and 500 μM of about 25% was detected in astrocytes from *GLAST*$^{+/-}$ mice compared to *GLAST*$^{+/+}$ astrocytes (Figure 4C). D-aspartate uptake was further decreased in astrocytes from *GLAST*$^{-/-}$ mice and residual uptake accounted for less than 40% of the uptake measured in *GLAST*$^{+/+}$ astrocytes at both 50 and 500 μM D-aspartate (Figure 4C). Glutamate was shown previously to cause an increase in glucose utilization and lactate production by astrocytes, a process known as aerobic glycolysis (Pellerin and Magistretti, 1994). We studied this metabolic response in cultured astrocytes obtained from *GLAST* mutant mice upon exposure to glutamate. Astrocytes from *GLAST*$^{+/+}$ mice responded strongly to glutamate with an increase in glucose utilization close to 75% above basal value (Figure 4D). In astrocytes from *GLAST*$^{+/-}$ mice however, the increase in glucose utilization triggered by glutamate was reduced by about half as compared to the response obtained in *GLAST*$^{+/+}$ astrocytes, while the effect of glutamate on glucose utilization in astrocytes from *GLAST*$^{-/-}$ mice was completely abolished (Figure 4D). In parallel, lactate production was affected in a very similar manner (Figure 4E).

Glutamate Transporter Expression Is Essential for Glutamate-Induced $[Na^+]_i$ Response in Astrocytes

Glutamate uptake through glutamate transporters proceeds via a cotransport with Na^+. In cultured astrocytes, glutamate transporter activity increases intracellular

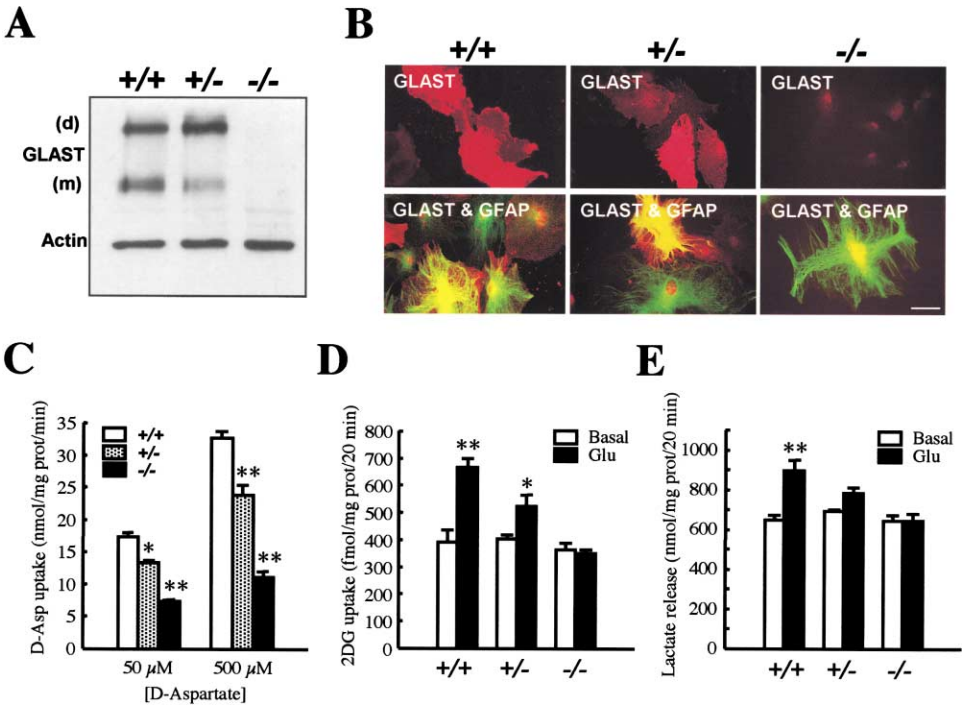

Figure 4. Enhancement of Glucose Utilization and Lactate Formation in Response to Glutamate Are Reduced in Parallel with Glutamate Uptake in Primary Cultures of Cortical Astrocytes from Neonatal *GLAST* Mutant Mice

(A) Immunoblot showing abundant GLAST expression in cultured cortical astrocytes from $GLAST^{+/+}$ and $GLAST^{+/-}$ mice. Expression was entirely absent in cells from $GLAST^{-/-}$ mice. GLT-1 expression was undetectable under these conditions (data not shown).

(B) Cortical astrocytes prepared from $GLAST^{+/+}$, $GLAST^{+/-}$, and $GLAST^{-/-}$ mice were immunohistochemically labeled with antibodies against GLAST (red) and GFAP (green). No positively stained cells could be found for GLAST in cultures from $GLAST^{-/-}$ mice while cells still retained expression of GFAP. Scale bar, 20 μm.

(C) Glutamate transport capacity was evaluated by measuring [^{3}H]-D-aspartate uptake in the presence of either 50 or 500 μM unlabeled D-aspartate. D-aspartate uptake decreased significantly in astrocytes from $GLAST^{+/-}$ mice and was reduced further in astrocytes from $GLAST^{-/-}$ mice at both 50 and 500 μM. Asterisks indicate a significant difference compared to $GLAST^{+/+}$ mice (Dunnett post hoc test, *$p < 0.05$, **$p < 0.01$). Data represent mean ± SEM, n = 3 of one representative experiment repeated three times with the same statistically significant results in every case.

(D and E) Glucose utilization by cultured astrocytes from *GLAST* mice was evaluated by measuring intracellular accumulation of [^{3}H]-2-deoxyglucose, while lactate production was determined by measuring lactate release in the medium. The effect of glutamate (Glu) at a concentration of 200 μM on glucose utilization (D) and lactate production (E) was reduced in astrocytes from $GLAST^{+/-}$ mice and abolished in astrocytes from $GLAST^{-/-}$ mice. Asterisks indicate a significant difference compared to basal condition (Student's t test, *$p < 0.05$, **$p < 0.01$). Data represent mean ± SEM, n = 3 of one representative experiment repeated from four to six times with the same statistically significant results in every case.

Na^+ concentration (Rose and Ransom, 1996; Chatton et al., 2000). The putative influence of modified glutamate transporter expression on glutamate-induced changes in intracellular sodium homeostasis was investigated by fluorescence microscopy. Exposure of astrocytes to 100 μM glutamate produced robust increases in intracellular Na^+ concentration (Figures 5A–5D) in cells from $GLAST^{+/+}$ mice. The intracellular Na^+ concentration was increased by 11.1 ± 1.2 mM in $GLAST^{+/+}$ astrocytes (Figure 5E). The increase was observed throughout the cell (Figure 5B) and was maintained as long as glutamate was applied. $[Na^+]_i$ rapidly recovered to baseline values after glutamate application ceased (Figure 5D). All cells examined produced a response. In $GLAST^{+/-}$ astrocytes, glutamate applied at a concentration of 100 μM produced responses that were significantly reduced as compared to $GLAST^{+/+}$ astrocytes (4.8 ± 1.2 mM, $p < 0.01$ versus $GLAST^{+/+}$; Figure 5E). Moreover, responses in astrocytes prepared from $GLAST^{-/-}$ mice were almost completely abolished (1.1 ± 0.1 mM, $p < 0.01$ versus $GLAST^{+/+}$; Figure 5F). No changes in the number of cells responding to the stimulus were observed nor the qualitative appearance of the response seemed modified. The only difference was in the extent of Na^+ concentration changes induced by glutamate.

Massive Na^+ Influx within Astrocytes Is the Major Determinant of the Metabolic Response to Glutamate

Reduced metabolic response to glutamate as observed in mutant mice could have arisen from unforeseen alterations in glial energy metabolism unrelated to the absence of glutamate transporter expression. Moreover, a more direct demonstration that Na^+ influx is the essential factor triggering the metabolic response was necessary. In order to assess the metabolic responsiveness of astrocytes from these mutant animals and test whether Na^+ influx is the necessary and sufficient condition to trigger the metabolic response, we attempted to rescue their metabolic response to glutamate by activat-

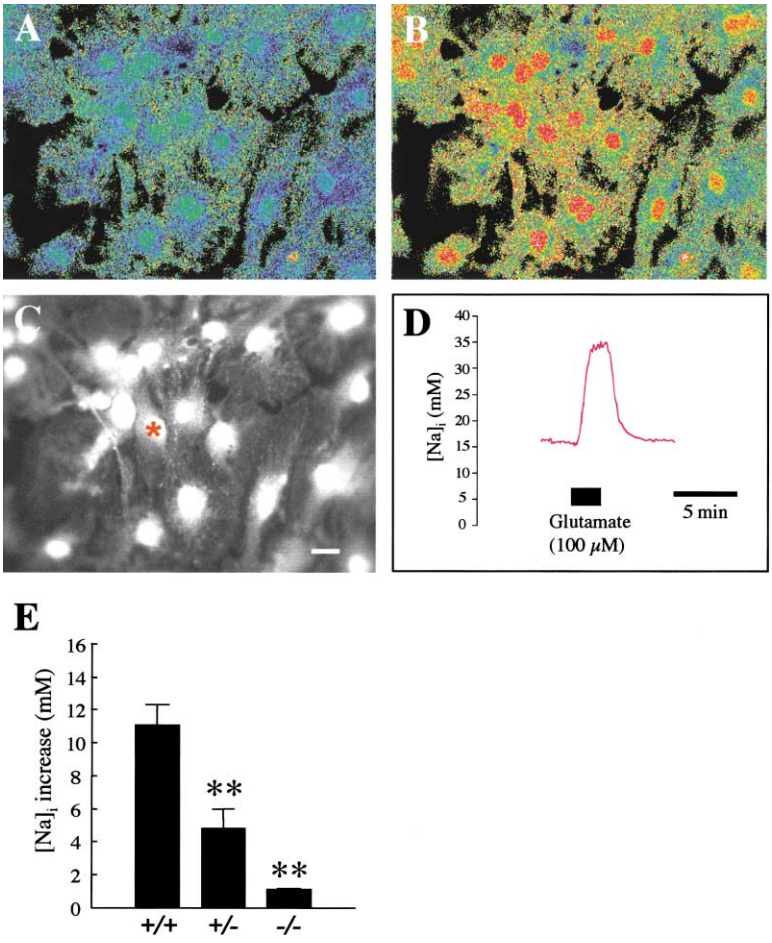

Figure 5. The $[Na^+]_i$ Response to Glutamate Is Strongly Reduced in Primary Cultures of Cortical Astrocytes from Neonatal *GLAST* Mutant Mice

(A) Pseudo-color SBFI (sodium binding benzofuran isophthalate) ratio image of mouse cortical astrocytes showing resting levels of intracellular Na^+.

(B) Increased intracellular Na^+ levels in the same preparation as in (A) upon exposure to 100 μM glutamate.

(C) Raw SBFI fluorescence image (excitation 380 nm) of cells in (A) and (B).

(D) Quantification of the $[Na^+]_i$ response evoked by 100 μM glutamate in the astrocyte labeled with an asterisk in (C). Fluorescence ratio values have been converted in Na^+ concentrations according to the calibration procedure described in Experimental Procedures.

(E) The increase in $[Na^+]_i$ induced by 100 μM glutamate was significantly reduced in astrocytes from *GLAST*$^{+/-}$ mice and almost completely abolished in astrocytes from *GLAST*$^{-/-}$ mice as compared to the response in *GLAST*$^{+/+}$ astrocytes. Asterisks indicate a significant difference compared to the same response in astrocytes from *GLAST*$^{+/+}$ mice (Dunnett post hoc test, $^{**}p < 0.01$). Data represent mean ± SEM, n = 6–38 cells from three to six different experiments.

ing an alternate pathway. It was previously shown that the drug cyclothiazide, an inhibitor of AMPA receptor desensitization, enhances glial Na^+ response to glutamate in a transporter-independent manner (Chatton et al., 2000). Here we observed that cyclothiazide restores the metabolic response to glutamate in astrocytes from *GLAST*$^{+/-}$ and *GLAST*$^{-/-}$ mice, leading to enhanced glucose utilization by about 2-fold as obtained in astrocytes from *GLAST*$^{+/+}$ mice (Figure 6A). In addition, cyclothiazide also restored to a similar level the enhancement in lactate production by astrocytes from *GLAST*$^{+/-}$ and *GLAST*$^{-/-}$ mice as compared to those of *GLAST*$^{+/+}$ mice (Figure 6B). The enhancement of glucose utilization obtained in astrocytes from *GLAST*$^{-/-}$ mice in the presence of glutamate and cyclothiazide could be entirely prevented by the ionotropic glutamate receptor antagonist CNQX, supporting the idea of an AMPA receptor-mediated effect in such case (Figure 6C). Finally, we took advantage of the fact that Li^+ can substitute for Na^+ and flow through AMPA receptor-mediated channels (Tong and Jahr, 1994), but is not efficiently pumped out by the Na^+/K^+ ATPase (Keynes and Swan, 1959) to assess the specific role of Na^+. First, it was observed that replacement of Na^+ by Li^+ in the medium reduced basal glucose utilization by about 60% (Figure 6D). Similar reductions in basal glucose utilization were observed previously when either Na^+ was replaced by choline or when ouabain was applied (Pellerin and Magistretti, 1994), thus confirming an involvement of the Na^+/K^+ ATPase in basal consumption. Finally, an enhancement of glucose utilization in astrocytes from *GLAST*$^{-/-}$ mice could be triggered by glutamate and cyclothiazide in a normal balanced salt solution medium, but it was abolished when Na^+ was replaced by Li^+ (Figure 6D).

Discussion

Impaired Metabolic Responses in *GLAST*$^{-/-}$ and *GLT-1*$^{-/-}$ Mice Do Not Arise from Developmental Delay or Alteration in Neurotransmission

Different explanations could potentially account for the reduced metabolic response upon activation in these mutant animals. First, as previously observed (Tanaka et al., 1997; K. Tanaka, unpublished data), we noticed that *GLT-1*$^{-/-}$ and *GLAST*$^{-/-}$ mice gained weight more slowly than did *GLT-1*$^{+/+}$ and *GLAST*$^{+/+}$ mice (data not shown). At P10, body weight of *GLAST*$^{-/-}$ and *GLT-1*$^{-/-}$ mice was significantly smaller compared to *GLAST*$^{+/+}$ and *GLT-1*$^{+/+}$ mice, respectively (−20%). Such a decrease in growth rate may have been the sign of a delay in maturation or other possible developmental perturbations that could in turn explain the relative metabolic unresponsiveness of mutant mice. Nissl staining on tangential sections from *GLAST*$^{-/-}$ or *GLT-1*$^{-/-}$ mice revealed the cytoarchitectural contours of individual bar-

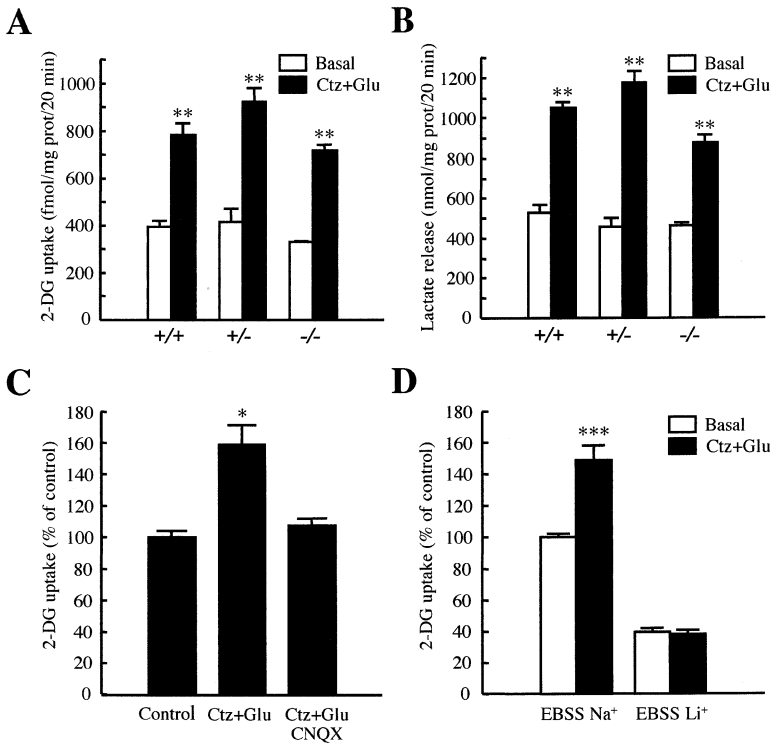

Figure 6. Cyclothiazide Restores the Metabolic Response Induced by Glutamate in Primary Cultures of Cortical Astrocytes from Neonatal *GLAST* Mutant Mice via an Ionotropic Glutamate Receptor-Mediated Na^+ Influx

The effect of glutamate at a concentration of 200 μM on both glucose utilization (A) and lactate formation (B) was studied in the presence of 100 μM cyclothiazide (Ctz), an inhibitor of AMPA receptor desensitization, in astrocytes from *GLAST* mutant mice. Asterisks indicate a significant difference compared to basal condition (Student's t test, $^{**}p < 0.01$). Data represent mean ± SEM, n = 3 for each condition. (C) Inhibition of glutamate-enhanced glucose utilization in presence of cyclothiazide by the ionotropic glutamate receptor antagonist CNQX (50 μM) in astrocytes from *GLAST*$^{-/-}$ mice. An asterisk indicates a significant difference compared to control condition (Dunnett post hoc test, $^{*}p < 0.05$). Data represent mean ± SEM, n = 3–4 for each condition. (D) Enhancement of glucose utilization in astrocytes from *GLAST*$^{-/-}$ mice induced by glutamate in the presence of cyclothiazide was abolished in an EBSS medium where Na^+ was replaced by Li^+. Asterisks indicate a significant difference compared to basal condition (Student's t test, $^{***}p < 0.001$). Data represent mean ± SEM, n = 4 for each condition.

rels typical of *GLAST*$^{+/+}$ and *GLT-1*$^{+/+}$ P10 mice. All major five rows (A–E) were clearly identified, with no visible modification of their shape (hollow, side, and septa). We also observed that in *GLAST*$^{-/-}$ and *GLT-1*$^{-/-}$ mice, cytochrome oxidase dense patches were organized into five rows in a similar orientation as in *GLAST*$^{+/+}$ and *GLT-1*$^{+/+}$ mice and with a similar density indicating that barrels from *GLAST*$^{-/-}$ and *GLT-1*$^{-/-}$ mice received functional thalamocortical afferents. Therefore, lack of expression of one or the other glial glutamate transporter does not appear to modify the cellular organization of the barrel field nor alter the expression of cytochrome oxidase indicating an apparently normal development of the whisker-to-barrel system.

Another possible explanation for the reduced metabolic response could be that excitability was altered in the somatosensory cortex of these mutant mice at P10. Measurement of basal 2-DG uptake and comparison between *GLAST*$^{+/+}$ and *GLAST*$^{-/-}$ mice as well as between *GLT-1*$^{+/+}$ and *GLT-1*$^{-/-}$ mice did not reveal any difference that would be consistent with enhanced excitability. Moreover, our immunoblot experiments indicated that levels of expression of both GluR1 and NR2A/B are unchanged in *GLT-1*$^{-/-}$ and *GLAST*$^{-/-}$ P10 mice. Since both AMPA and NMDA receptor currents largely contribute to thalamocortical synaptic responses in the developing mouse (Lu et al., 2001), it is unlikely that a major alteration of glutamatergic transmission occurred in these mice. Despite the fact that we cannot definitively rule out this possibility, electrophysiological results obtained so far in adult mice suggest otherwise. Indeed, the decay of EPSCs measured in the hippocampus or in the cerebellum is not significantly modified in adult *GLT-1*$^{-/-}$ and *GLAST*$^{-/-}$ mice (Watase et al., 1998; Tanaka et al., 1997), suggesting that glutamatergic neurotransmission is preserved in these mice despite an alteration of the clearance of glutamate from the synaptic cleft. We have also provided evidence previously that a normal whisker-related neuronal activity was still observed in the somatosensory cortex 24 hr after downregulating GLAST via injection of GLAST antisense oligonucleotides in adult rats (Cholet et al., 2001). In immature mutant mice, at a time when GLAST and GLT-1 display a similar level of expression, it is likely that part of glutamate transport is preserved and carried out by the other nontargeted transporter. Therefore, P10 *GLAST*$^{-/-}$ and *GLT-1*$^{-/-}$ mice may still have sufficient residual glutamate transport capacity to supply neurons with the precursor glutamine, as evidenced by the unchanged level of expression of glutamine synthetase in these animals. In addition, in mice at P10, no significant pathological events due to elevated levels of residual glutamate (cell death and epilepsy) have yet occurred as described in the adult *GLT-1*$^{-/-}$ mice (Tanaka et al., 1997), such that glutamatergic neurotransmission is most likely undisturbed at that stage.

Role of Astrocytes and Their Glutamate Transporters in Coupling the Observed Metabolic Response to Neuronal Activation

Our immunohistochemical observation that both glial glutamate transporters GLAST and GLT-1 are selectively and prominently expressed in the barrel cortex at P10 could be broadly related to the major role played by excitatory amino acid transmission in both development and plasticity of the somatosensory barrel cortex (Erzurumlu and Kind, 2001). In view of our 2-DG data however, it is proposed that glial glutamate transporters are also

required for an appropriate metabolic response to neuronal activation in the whisker-to-barrel pathway of P10 mice. This idea is reinforced by our observation in vivo using NMDA and non-NMDA receptor antagonists that activation of glutamatergic receptors cannot explain the enhancement of glucose utilization. Preparations of cortical astrocytes in vitro provided a unique opportunity to further investigate the cellular and molecular mechanism linking glutamate transport to enhanced glucose utilization. We took advantage of the fact that GLAST expression predominates in cultured astrocytes and that there is virtually no contribution from GLT-1 to the overall glutamate uptake (Stanimirovic et al., 1999) to investigate the coupling mechanism in astrocytes from *GLAST* mutant mice. Thus, as the expression of GLAST was reduced in astrocytes from *GLAST*$^{+/-}$ and GLAST$^{-/-}$ mice, a parallel decrease in glutamate uptake and in glutamate-induced glucose utilization as well as lactate formation was observed. This situation is analogous to previous observations showing that the nonspecific glutamate transporter inhibitors *threo*-β-hydroxyaspartate and L-CCGIII prevented the enhancement of aerobic glycolysis (i.e., glucose utilization and lactate release) induced by glutamate in cultured cortical astrocytes (Pellerin and Magistretti, 1994). These data indicate clearly that a link exists between glutamate uptake capacity in astrocytes (as controlled by GLAST here) and their ability to metabolically respond to glutamate. Even if this point could not be directly addressed in vitro, it is likely that a similar relationship exists with the other glial glutamate transporter GLT-1. This is particularly relevant since the expression of both glial glutamate transporters varies during development, with GLAST being predominant in the cortex during the first postnatal week, while GLT-1 expression increases during the second week to become the major transporter thereafter (Furuta et al., 1997). Thus, it is postulated that the contribution of each glial glutamate transporter to the overall glutamate uptake capacity as well as to the metabolic response of astrocytes might vary depending of the developmental stage.

Since GLAST and GLT-1 are almost exclusively located on astrocytes (Danbolt, 2001), results reported here strongly suggest a significant role of these glial cells in coupling physiological activation with energy metabolism in vivo. Indeed, a close examination of anatomical as well as functional characteristics of astrocytes argues in favor of a central role for these cells in coupling neuronal activity to glucose utilization. Our recent anatomical data demonstrating a clear relationship between perivascular astrocyte endfeet and the endothelial glucose transporter (GLUT1) strongly supports this contention (Kacem et al., 1998). As astrocytes also display processes ensheathing synapses (Grosche et al., 1999), these cells are ideally positioned to sense synaptic activity and to couple it to glucose uptake. Our combined in vivo and in vitro experiments suggest that (1) brain glucose metabolism is closely linked to glutamatergic neuronal activity, and (2) astrocytes are one of the key elements of the metabolic coupling. The notion that brain glucose metabolism is related to glutamatergic neuronal activity has been substantiated by a magnetic resonance spectroscopy study indicating a stoichiometry of 1:1 between glutamate recycling (via its uptake and transformation into glutamine within astrocytes) and oxidative glucose metabolism (Sibson et al., 1998).

Intracellular Na^+ Concentration Changes within Astrocytes Serve as a Signal to Trigger Aerobic Glycolysis

Glutamate transporters operate by coupling glutamate transport with the Na^+ gradient. In addition, they obey a precise stoichiometry. For each glutamate molecule transported within the cell, three Na^+ ions are cotransported together with one proton while one K^+ ion is extruded (Danbolt, 2001). As a consequence, a significant Na^+ influx occurs in astrocytes, which is evidenced by the generation of a glial inward current (Bergles and Jahr, 1997) and accumulation of $^{22}Na^+$ inside the cell (Kimelberg et al., 1989). Glutamate uptake also leads to important changes in intracellular Na^+ concentration as measured by fluorescence microscopy (Rose and Ransom, 1996; Chatton et al., 2000). Our data further confirm that the increase in intracellular Na^+ concentration induced by glutamate is directly related to glutamate transport capacity (via GLAST expression) in cultured astrocytes. In addition, it is suggested that variations in intracellular Na^+ concentration could constitute a new form of intracellular signaling allowing astrocytes to detect enhanced synaptic activity at glutamatergic synapses.

What could be the molecular processes sensitive to such fluctuations in intracellular Na^+ concentration? Stimulation of Na^+ entry in cells by various means was demonstrated previously to stimulate Na^+/K^+ ATPase activity (Mendoza et al., 1980). Moreover, a close association between Na^+/K^+ ATPase activity and activation of glycolysis has been demonstrated in numerous cell types (Parker and Hoffman, 1967; Paul et al., 1979), including astrocytes (Yarowsky et al., 1986). In astrocytes indeed, it was previously shown that glutamate uptake leads to enhanced Na^+/K^+ ATPase activity, most likely as a consequence of the elevation of intracellular Na^+ concentration (Pellerin and Magistretti, 1997). In addition, it was suggested that increased Na^+/K^+ ATPase activity would be responsible for the activation of aerobic glycolysis in this cell type. Our results showing the disappearance of both enhanced glucose utilization and lactate production in astrocytes from GLAST mutant mice upon exposure to glutamate would be perfectly consistent with this concept.

This conclusion is further substantiated by the results obtained with cyclothiazide. Cyclothiazide is a drug that prevents desensitization of AMPA receptors (Yamada and Tang, 1993). As a consequence, it enhances the amount of Na^+ that enters the cell through these activated AMPA receptors and then causes a significant elevation of intracellular Na^+ levels (Chatton et al., 2000). The fact that cyclothiazide completely restored the effect of glutamate on both glucose utilization and lactate production in astrocytes prepared from *GLAST*$^{-/-}$ mice leads to two important conclusions. First, it demonstrates that the absence of a metabolic response to glutamate in these cells is not a consequence of some unspecific metabolic disturbances in such mutant animals. Second, it further emphasizes the crucial role of

Na^+ in mediating this metabolic effect. It indicates that it is not the entry route of Na^+ however, but rather, its consequence which is responsible for the metabolic response observed in astrocytes. In this regard, replacement of Na^+ by Li^+ in the medium clearly demonstrates that Na^+ removal via the Na^+/K^+ ATPase remains the critical step leading to the metabolic response, regardless of the mode of Na^+ entry.

Significance of Neuron-Glia Metabolic Crosstalk

Glucose is considered the major if not exclusive energy substrate provided by the circulation to the adult brain. Moreover, glucose utilization has been considered a direct reflection of neuronal activity since it has been assumed that glucose consumption occurs almost exclusively in neurons to fulfill energy needs of activated neurons that have to reestablish their ion gradients. This assumption has formed the basis for the development of brain imaging techniques relying on the accumulation of the glucose analog 2-deoxyglucose. Although the general concept remains valid, the picture that is now emerging at the cellular and molecular levels might lead to some reevaluation of our understanding of these events. Thus, as our results and those of others have revealed, astrocytes might contribute significantly to the glucose utilization signal. Moreover, activation of aerobic glycolysis in astrocytes leads to the formation and release of lactate. Since numerous evidence indicate that lactate is a potential energy substrate for neurons (Ames, 2000), this opens up new perspectives for brain energetics. Although these observations do not preclude glucose utilization by neurons, it simply reveals new and more intricate aspects of brain energy metabolism. In addition, even if a significant portion of glucose utilization was taking place in astrocytes, it would remain normally proportional to neuronal activity. There might be some situations however where this direct relationship could be modified. In such cases, brain images would be misleading and might not necessarily reflect neuronal activity. This final point underlines the importance of understanding the cellular and molecular mechanisms giving rise to the signals used in brain imaging in order to make correct interpretations and diagnosis (Magistretti and Pellerin, 1999; Bonvento et al., 2002).

Experimental Procedures

Animals

Pups were obtained either from pregnant C57 BL/6 mice (Janvier, France) or from C57BL/6 *GLAST*$^{+/-}$ and *GLT-1*$^{+/-}$ heterozygote breeder pairs (Tanaka et al., 1997; Watase et al., 1998). Animals were maintained under standard conditions of feeding and lighting (12/12 hr light-darkness cycle, 22°C). Experimental protocols were approved by the Bureau de la Protection Animale of the Ministère de l'Agriculture (Authorization number 75-01 to G.B.). For each experiment, all littermates were processed, and their individual genotype was determined a posteriori by PCR as previously described (Tanaka et al., 1997; Watase et al., 1998).

Immunohistochemistry on Cortical Sections

Brains from P10 animals were removed and immersed in 4% paraformaldehyde in 0.1 M phosphate buffer (PB) at pH 7.4 for 24 hr. Brain tissue was cryoprotected in 20% sucrose in 0.1 M PB at pH 7.4 for 24 hr. The forebrain was bisected midsagittally, and each hemisphere was fit to a small plastic wedge allowing tangential cutting of the barrel field. Tissue plus wedge were immersed and frozen in isopentane at about −40°C. They were mounted onto a cryostat object holder with cooled embedding matrix (M-1, Lipshaw). Each midhemisphere was processed for GLAST/GLT-1 immunohistochemistry. The tangential sections were pretreated with 0.3% H_2O_2 in phosphate buffer saline (PBS, 0.02 M, pH 7.4) for 15 min, rinsed in PBS, and incubated sequentially in 5% normal goat serum in PBS for blocking (1 hr), with the primary antibody (0.1 μg/ml GLAST or GLT-1) (Shibata et al., 1997; Yamada et al., 1998) together with 2% normal goat serum and 0.1% Tween-20 in PBS (12 hr), with the secondary antibody (biotinylated goat anti-rabbit IgG) diluted at 1:200 with 0.1% Tween-20 in PBS for 1 hr, and then with avidin-biotin complex diluted at 1:200 for 1 hr (Vector Laboratories). Diaminobenzidine tetrahydrochloride with H_2O_2 was used as peroxidase substrate to visualize sites of antibody binding.

Immunoblotting

Fresh frozen samples of mice cortex at P10 were briefly sonicated in 50 mM Tris-HCl, 1% sodium dodecyl sulfate (SDS), and 100 mM NaCl with protease inhibitors (1697498-Boehringer) in a total volume of 600 μl. The homogenate was centrifuged at 13,000 × g (20 min at 4°C), and the supernatant was collected. Astrocyte cultures were homogenized in a buffer containing 62.5 mM Tris-HCl, 50 mM dithiotreitol (DTT), 0.3% sodium dodecylsulfate (SDS), and a mixture of protease inhibitors (10 μg/ml of each, antipapain, leupeptin, pepstatin A, and E64, and 1 mM phenylmethylsulfonylfluoride (Sigma; A6191, L9783, P5318, E3132, and P7626). Protein concentrations were determined by the method of Lowry (Lowry et al., 1951) using bovine serum albumin as standard. Sample was added (vol/vol) with buffer (63 mM Tris-HCl, pH 6.8, 2% sodium dodecyl sulfate, 1% glycerol, 0.05% bromophenol Blue and 5% 2-Mercaptoethanol). Electrophoresis of total proteins was performed on a SDS-polyacrylamide gel (12% acrylamide/bisacrylamide, Sigma). Proteins were transferred to PVDF membrane (Biorad) with buffer (25 mM Tris-HCl, pH 8.3, 20% methanol, 0.1% SDS, 192 mM glycine) by electroblotting during 1 hr. Blots were blocked with 5% nonfat dry milk in TBST (20 mM Tris-HCl, pH 7.5, 500 mM NaCl, 0.1% Tween-20) at room temperature and then incubated with different primary antibodies: actin (42 kDa; 1/2000) (A2066 Sigma), GLAST (65 kDa), GLT-1 (67 kDa; 0.05 μg /ml) (same origin as above), EAAC1 (69 kDa; 1/2000) (Alpha Diagnostic), glutamine synthetase (45 kDa; 1/2000) (Transduction laboratories), GluR1 (105 kDa; 1/100) (Sigma), and NR2A/B (179 kDa; 1/200) (Chemicon) overnight at 4°C. After primary antibody incubation, membranes were washed and incubated with peroxydase-conjugated secondary antibodies (1/2000) and developed with ECL (PPN 2108-Amersham) using Kodak X-OMAT film. The resulting bands were digitized, and immunoreactive proteins were semiquantitatively evaluated by densitometry. For semiquantitative evaluation of the relative level of expression of all proteins, the optical density was normalized to the optical density of actin in each animal.

Whisker Stimulation and In Vivo ^{14}C-2-Deoxyglucose (^{14}C-2-DG) Uptake

Ten-day-old mice (P10) were gently restrained, and all whiskers except the two caudal whiskers of row C (C1C2) of both whiskerpads were clipped. Mu metal pieces (1.5 mm long, 0.2 mm diameter) were fastened onto C1C2 whiskers of one or both sides with cyanoacrylic glue. Mice were immobilized on a support and received an i.p. injection of 2-[1-^{14}C]deoxy-D-glucose (16.5 μCi/100 g body weight) (NEN, NEC495) in NaCl 0.9%. They were then immediately placed in the Lausanne whisker stimulator as previously described (Melzer et al., 1985). Some C57BL/6 mice received an i.p. injection of MK-801 (0.05 mg/kg) or NBQX (20 mg/kg) 10 min before 2-DG administration. The stimulation consisted of magnetic field bursts that were delivered at 50 Hz, the burst duration was 46 ms, and the interval between bursts was 90 ms. 45 min after 2-DG injection, brains were removed and frozen in isopentane at −40°C. Sections were cut coronally or tangentially to the barrel field at 20 μm, mounted on slides, and dried on a 60°C hot plate. Slides were then processed for autoradiography together with calibrated [^{14}C]-standards (American Radiolabeled Chemicals) on BIOMAX film (Kodak) for 9–10 days at room temperature. Autoradiograms were digitized and analyzed using a computer-based image analysis system (Biocom 2000, France). Gray levels

determined on the autoradiograms were calibrated using the coexposed densitometric microscales and converted to nCi/g tissue. The [^{14}C] concentration was determined within regions of interest (ROIs) depicting the barrels C1 and C2. A mean 2-DG uptake was calculated from all densitometric values measured in a consecutive series of sections (four to six) that contained these barrels. For each animal, a reference value (background) was calculated as the mean 2-DG uptake in unstimulated barrels measured in the same consecutive series of sections. This reference value was used to calculate the relative 2-DG uptake using the formula: relative 2-DG uptake = (2-DG uptake − reference value)/reference value. This value, expressed as a percentage, was determined in each hemibrain. Pseudocolored images were generated by replacing the range of 256 gray level values with 16 colors. The correspondence between the color code and the 2-DG uptake is presented (in nCi/g tissue) with each case on a scale.

Primary Cultures of Neonatal Mouse Cerebral Cortical Astrocytes

Primary cultures of cerebral cortical astrocytes were prepared from newborn mice (1–2 days old) as previously described (Pellerin and Magistretti, 1994). Briefly, forebrains were removed from skulls and placed in ice-cold DMEM (Sigma D-7777) containing 25 mM glucose and supplemented with 10% fetal calf serum (Fakola, Switzerland), 44 mM $NaHCO_3$, and 10 ml/l of an antibiotic, antimycotic solution (Sigma A-7292) (DMEM-FCS). After careful dissection of neocortices, cells were dissociated by passage of neocortices through needles of decreasing gauges (1.2 × 40 mm, 0.8 × 40 mm, and 0.5 × 16 mm) with a 10 ml syringe. No trypsin was used for dissociation. Cells were seeded at a density of 10^5/cm^2 on 35 × 10 mm Petri dishes or 30 mm poly-ornithine-coated glass coverslips in DMEM-FCS and were incubated at 37°C in a water-saturated atmosphere containing 5% CO_2/95% air. 5 days after seeding, cells were washed with DMEM-FCS, and subsequently the medium was replaced every 2–3 days. Cultures were used for experiments at confluence, usually between 19 and 22 days after seeding. This procedure yields cultures that are over 95% immunoreactive for glial fibrillary acidic protein. All experiments were carried out on cultures from *GLAST*$^{+/+}$, *GLAST*$^{+/-}$, and *GLAST*$^{-/-}$ littermates for direct comparison and repeated on cultures from separate series of neonates.

Immunohistochemistry on Cultured Astrocytes

Cultures were fixed with a solution of 4% paraformaldehyde in phosphate-buffered saline (PBS, 0.1 M, pH 7.4, 25 min, 4°C). They were treated with 4% normal donkey serum in PBS containing 0.2% Triton X-100 (1 hr, room temperature) to reduce nonspecific binding of antibodies. For single labeling, cultures were incubated overnight at 4°C in a solution containing a rabbit polyclonal anti-GLAST antibody (Shibata et al., 1997), diluted 1/4000. For double immunolabeling, cultures were incubated in solutions containing an anti-GLAST antibody (diluted 1/4000) and a mouse monoclonal anti-GFAP (Sigma), diluted 1/800 (overnight, 4°C). All antibodies were diluted in PBS. After washing in PBS, cultures were treated with appropriate fluorescent conjugates (30 min, room temperature). Anti-rabbit Igs conjugated to Cy3 (diluted 1/800, Jackson Immunoresearch Laboratories) served to identify GLAST; anti-mouse Igs conjugated to fluorescein isothiocyanate (FITC, 1/500, Jackson Immunoresearch Laboratories) served to visualize GFAP. The cultures were mounted with fluoromount (Vectashield, Vector Laboratories Inc.) and examined with an epifluorescence microscope (Zeiss Axioplan) with appropriate filters.

^{3}H-D-Aspartate (^{3}H-D-Asp) Uptake Measurement

Glutamate transport capacity was determined by measuring ^{3}H-D-Asp uptake as described previously (Debernardi et al., 1999). On the day of the experiment, the culture medium was replaced by serum-free DMEM (Sigma D5030) supplemented with 5 mM glucose, 44 mM $NaHCO_3$, 10 ml/l of an antibiotic, antimycotic solution (Sigma A-7292), and 0.045 mM phenol red ($DMEM_5$). Cells were incubated for 2 hr at 37°C in a water-saturated atmosphere containing 5% CO_2/95% air. The medium was then replaced by 2 ml of the same $DMEM_5$ medium containing ^{3}H-D-Asp (American Radiolabeled Chemicals) at a tracer concentration of 1 μCi/ml (specific activity 18.5 Ci/mmol) and unlabeled D-Asp at either 50 or 500 μM. Cells were incubated for 5 min, a period of time during which D-Asp uptake is known to be linear. Reaction was stopped by transfer of dishes on ice, aspiration of the medium, rinsing cells three times with ice-cold PBS, and addition of 2 ml of 0.01 N NaOH containing 0.1% Triton X-100 to lyse cells. Aliquots of 500 μl were assayed for radioactivity by liquid scintillation counting, while 50 μl aliquots were used for measurement of protein content by the method of Bradford (1976). Results, which represent transporter-mediated glutamate uptake, were calculated by subtracting from total counts the portion that was not inhibited by incubation at 4°C (nontransporter-mediated uptake). Transporter-mediated uptake accounted for approximately 90%–95% of total uptake. Total D-Asp transport can be calculated from intracellular [^{3}H-D-Asp], extracellular [^{3}H-D-Asp], and extracellular [D-Asp].

In Vitro ^{3}H-2-Deoxyglucose Uptake and Phosphorylation Measurement

Glucose utilization was determined by measuring ^{3}H-2-DG uptake and phosphorylation as previously described (Pellerin and Magistretti, 1994). The procedure is similar to the one described above for D-Asp uptake measurement except that ^{3}H-2-DG (American Radiolabeled Chemicals) at a concencentration of 1 μCi/ml (specific activity 60 Ci/mmol) was used as a tracer instead of ^{3}H-D-Asp. Moreover, incubation time was 20 min instead of 5 min. In experiments where Na^+ was replaced by Li^+ in the incubation medium, an Earle's Balanced Salt Solution (EBSS) with the following composition was used: 4.62 mM KCl, 1.3 mM $CaCl_2$, 0.81 mM $MgSO_4$, 0.78 mM KH_2PO_4, 25 mM $CholineHCO_3$, 5 mM glucose, and 160 mM NaCl or 160 mM LiCl. Just prior to glucose utilization measurement, cells preincubated in $DMEM_5$ medium were rinsed once with appropriate EBSS medium, and then the same medium containing the radioactive tracer was added. Glutamate and cyclothiazide (Tocris) were added together with the medium containing the tracer while cytochalasin B (Sigma) was added 20 min prior to, as well as during, incubation with the tracer. CNQX (Tocris) was added at the same time as glutamate and cyclothiazide. Results, which represent glucose transporter-mediated uptake and subsequent phosphorylation, were calculated by subtracting from total counts the portion that was not inhibited by the glucose transporter inhibitor cytochalasin B at 25 μM. Cytochalasin-sensitive uptake usually accounted for approximately 80% of total uptake.

Lactate Release Assay

Lactate release measurements were performed as previously described (Pellerin and Magistretti, 1994). The same preincubation procedure as described above for 2-DG uptake measurement was used except that phenol red was omitted from $DMEM_5$. Cells were then incubated for 30 min in the same conditions as above in $DMEM_5$ without phenol red. The reaction was stopped by collecting the medium on ice. 2 ml of 0.01 N NaOH + 0.1% Triton were added to lyse the cells. 50 μl aliquots were used for protein measurement. Lactate release into the medium was measured enzymatically by an enzymatic-spectrophotometric method. To a 200 μl aliquot, 1 ml of a glycine-semicarbazide 0.2 M, pH 10, buffer containing 0.003 M NAD (Boehringer) and LDH ~14 U/ml (Boehringer) was added. Samples were incubated at 40°C for 1 hr. After samples cooled down to room temperature, their absorbance was read at 340 nm and absolute values determined from a standard curve.

$[Na^+]_i$ Measurement

$[Na^+]_i$ measurements were carried out on the stage of an inverted epifluorescence microscope (Zeiss) and observed through a 40× 1.3 N.A. oil-immersion Neofluar objective lens (Zeiss). Fluorescence excitation wavelengths were selected using a holographic monochromator (Till Photonics, Germany), and fluorescence was detected using a 12-bit cooled CCD camera (Princeton Instruments, NJ). Acquisition of images as well as time series were computer controlled using the software Metafluor (Universal Imaging, PA). $[Na^+]_i$ was measured in single cells grown on glass coverslips after loading the cells with the Na^+-sensitive fluorescent dye sodium binding benzofuran isophthalate (SBFI-AM, Teflabs, TX). Cell loading was performed at 37°C using 15 μM SBFI-AM in a HEPES-

buffered balanced solution (see composition below). Once loaded with SBFI, cells were placed in a thermostated perfusion chamber and superfused at 35°C. Fluorescence was sequentially excited at 340 and 380 nm and detected through a 510 nm bandpass filter (80 nm bandwidth). Fluorescence excitation ratios (F_{340nm}/F_{380nm}) were computed for each image pixel and produced ratio images of cells that were proportional with $[Na^+]_i$. In situ calibration was performed after each experiment using a protocol previously described (Chatton et al., 2000). Briefly, cells were permeabilized for monovalent cations using 6 μg/ml gramicidin and 10 μM monensin with simultaneous inhibition the Na^+/K^+-ATPase using 1 mM ouabain. Cells were then sequentially perfused with solutions buffered at pH 7.2 with 20 mM HEPES and containing 0, 5, 10, 20, and 50 mM Na^+, respectively, and 30 mM Cl^-, 136 mM gluconate with a constant total concentration of Na^+ and K^+ of 165 mM. A five-point calibration curve was computed for each selected cell in the field of view and used to convert fluorescence ratio values (F_{340nm}/F_{380nm}) into Na^+ concentrations. Experimental solutions contained: 135 mM NaCl, 5.4 mM KCl, 25 mM $NaHCO_3$, 1.3 mM $CaCl_2$, 0.8 mM $MgSO_4$, 0.78 mM NaH_2PO_4, and 5 mM glucose, bubbled with 5% CO_2/95% air. The solution for dye-loading contained: 135 mM NaCl, 5.4 mM KCl, 20 mM HEPES, 1.3 mM $CaCl_2$, 0.8 mM $MgSO_4$, 0.78 mM NaH_2PO_4, and 20 mM glucose and was supplemented with 0.1% Pluronic F-127 (Molecular Probes).

Acknowledgments

The authors acknowledge the expert technical assistance provided by Mauricette Maillard, Didier Foretay, Charles Quairiaux, and Angélique Regnier. They also thank Ruth Debernardi for preparing astrocyte culture homogenates for Western blotting, Jean-François Brunet for performing RT-PCR of glutamate transporters, and Sylvain Lengacher for setting up genotyping. We are also grateful to Igor Allaman and Karin Pierre for critically reading the manuscript. This work was supported by a Human Frontier Science Program grant number RG118/1998-B (to L.P. and G.B.).

Received: March 6, 2002
Revised: November 26, 2002

References

Ames, A., III. (2000). CNS energy metabolism as related to function. Brain Res. Rev. *34*, 42–68.

Andriezen, W.L. (1893). On a system of fibre-like cells surrounding the blood vessels of the brain of man and mammals, and its physiological significance. Int. Monatsschr. Anat. Physiol. *10*, 532–540.

Araque, A., Parpura, V., Sanzgiri, R.P., and Haydon, P.G. (1998). Glutamate-dependent astrocyte modulation of synaptic transmission between cultured hippocampal neurons. Eur. J. Neurosci. *10*, 2129–2142.

Bergles, D.E., and Jahr, C.E. (1997). Synaptic activation of glutamate transporters in hippocampal astrocytes. Neuron *19*, 1297–1308.

Bonvento, G., Sibson, N., and Pellerin, L. (2002). Does glutamate image your thoughts? Trends Neurosci. *25*, 359–364.

Bradford, M.M. (1976). A rapid and sensitive method for the quantitation of microgram quantities of protein utilizing the principle of protein-dye binding. Anal. Biochem. *72*, 248–254.

Chatton, J.-Y., Marquet, P., and Magistretti, P.J. (2000). A quantitative analysis of L-glutamate-regulated Na^+ dynamics in mouse cortical astrocytes : implications for cellular bioenergetics. Eur. J. Neurosci. *12*, 3843–3853.

Cholet, N., Pellerin, L., Welker, E., Lacombe, P., Seylaz, J., Magistretti, P., and Bonvento, G. (2001). Local injection of antisense oligonucleotides targeted to the glial glutamate transporter GLAST decreases the metabolic response to somatosensory activation. J. Cereb. Blood Flow Metab. *21*, 404–412.

Danbolt, N.C. (2001). Glutamate uptake. Prog. Neurobiol. *65*, 1–105.

Debernardi, R., Magistretti, P.J., and Pellerin, L. (1999). Trans-inhibition of glutamate transport prevents excitatory amino acid-induced glycolysis in astrocytes. Brain Res. *850*, 39–46.

Erzurumlu, R.S., and Kind, P.C. (2001). Neural activity: sculptor of 'barrels' in the neocortex. Trends Neurosci. *24*, 589–595.

Furuta, A., Rothstein, J.D., and Martin, L.J. (1997). Glutamate transporter protein subtypes are expressed differentially during rat CNS development. J. Neurosci. *17*, 8363–8375.

Gallo, V., and Ghiani, C.A. (2000). Glutamate receptors in glia: new cells, new inputs and new functions. Trends Pharmacol. Sci. *21*, 252–257.

Grosche, J., Matyash, V., Möller, T., Verkhratsky, A., Reichenbach, A., and Kettenmann, H. (1999). Microdomains for neuron-glia interaction:parallel fiber signaling to Bergmann glial cells. Nat. Neurosci. *2*, 139–143.

Haugeto, O., Ullensvang, K., Levy, L.M., Chaudhry, F.A., Honore, T., Nielsen, M., Lehre, K.P., and Danbolt, N.C. (1996). Brain glutamate transporter proteins form homomultimers. J. Biol. Chem. *271*, 27715–27722.

Kacem, K., Lacombe, P., Seylaz, J., and Bonvento, G. (1998). Structural organization of the perivascular astrocyte endfeet and their relationship with the endothelial glucose transporter: a confocal microscopy study. Glia *23*, 1–10.

Keynes, R.D., and Swan, R.C. (1959). The permeability of frog muscle fibres to lithium ions. J. Physiol. *147*, 626–638.

Kim, W.T., Rioult, M.G., and Cornell-Bell, A.H. (1994). Glutamate-induced calcium signaling in astrocytes. Glia *11*, 173–184.

Kimelberg, H.K., Pang, S., and Treble, D.H. (1989). Excitatory amino acid-stimulated uptake of $^{22}Na^+$ in primary astrocyte cultures. J. Neurosci. *9*, 1141–1149.

Lu, H.C., Gonzalez, E., and Crair, M.C. (2001). Barrel cortex critical period plasticity is independent of changes in NMDA receptor subunit composition. Neuron *32*, 619–634.

Lowry, O.H., Rosebrough, H.J., Farr, A.L., and Randall, R.J. (1951). Protein measurement with the Folin phenol reagent. J. Biol. Chem. *193*, 265–275.

Magistretti, P.J., and Pellerin, L. (1999). Cellular mechanisms of brain energy metabolism and their relevance to functional brain imaging. Philos. Trans. R. Soc. Lond. B Biol. Sci. *354*, 1155–1163.

Magistretti, P.J., Pellerin, L., Rothman, D.L., and Shulman, R.G. (1999). Energy on demand. Science *283*, 496–497.

Melzer, P., Van der Loos, H., Dörfl, J., Welker, E., Robert, P., Emery, D., and Berrini, J.C. (1985). A magnetic device to stimulate selected whiskers of freely moving or restrained small rodents: its application in a deoxyglucose study. Brain Res. *348*, 229–240.

Melzer, P., Welker, E., Dörfl, J., and Van der Loos, H. (1994). Maturation of the neuronal metabolic response to vibrissa stimulation in the developing whisker-to-barrel pathway of the mouse. Dev. Brain Res. *77*, 227–250.

Mendoza, S.A., Wigglesworth, N.M., and Rozengurt, E. (1980). Vasopressin rapidly stimulates Na entry and Na-K pump activity in quiescent cultures of mouse 3T3 cells. J. Cell. Physiol. *105*, 153–162.

Morgello, S., Uson, R.R., Schwartz, E.J., and Haber, R.S. (1995). The human blood-brain barrier glucose transporter (GLUT1) is a glucose transporter of gray matter astrocytes. Glia *14*, 43–54.

Newman, E.A., and Zahs, K.R. (1998). Modulation of neuronal activity by glial cells in the retina. J. Neurosci. *18*, 4022–4028.

Parker, J.C., and Hoffman, J.F. (1967). The role of membrane phosphoglycerate kinase in the control of glycolytic rate by active cation transport in human red blood cells. J. Gen. Physiol. *50*, 893–916.

Paul, R., Bauer, M., and Pease, W. (1979). Vascular smooth muscle: aerobic glycolysis linked to sodium and potassium transport processes. Science *206*, 1414–1416.

Pellerin, L., and Magistretti, P.J. (1994). Glutamate uptake into astrocytes stimulates aerobic glycolysis : a mechanism coupling neuronal activity to glucose utilization. Proc. Natl. Acad. Sci. USA *91*, 10625–10629.

Pellerin, L., and Magistretti, P.J. (1997). Glutamate uptake stimulates Na^+, K^+-ATPase activity in astrocytes via activation of a distinct subunit highly sensitive to ouabain. J. Neurochem. *69*, 2132–2137.

Pfrieger, F.W., and Barres, B.A. (1997). Synaptic efficacy enhanced by glial cells in vitro. Science *277*, 1684–1687.

Poitry-Yamate, C.L., Poitry, S., and Tsacopoulos, M. (1995). Lactate released by Müller glial cells is metabolized by photoreceptors from mammalian retina. J. Neurosci. *15*, 5179–5191.

Robitaille, R. (1998). Modulation of synaptic efficacy and synaptic depression by glial cells at the frog neuromuscular junction. Neuron *21*, 847–855.

Rose, C.R., and Ransom, B.R. (1996). Mechanisms of H^+ and Na^+ changes induced by glutamate, kainate, and D-aspartate in rat hippocampal astrocytes. J. Neurosci. *16*, 5393–5404.

Shibata, T., Yamada, K., Watanabe, M., Ikenaka, K., Wada, K., Tanaka, K., and Inoue, Y. (1997). Glutamate transporter GLAST is expressed in the radial glia-astrocyte lineage of developing mouse spinal cord. J. Neurosci. *17*, 9212–9219.

Sibson, N.R., Dhankhar, A., Mason, G.F., Rothman, D.L., Behar, K.L., and Shulman, R.G. (1998). Stoichiometric coupling of brain glucose metabolism and glutamatergic neuronal activity. Proc. Natl. Acad. Sci. USA *95*, 316–321.

Sibson, N.R., Mason, G.F., Shen, J., Cline, G.W., Herskovits, A.Z., Wall, J.E.M., Behar, K.L., Rothman, D.L., and Shulman, R.G. (2001). In vivo ^{13}C NMR measurement of neurotransmitter glutamate cycling, anaplerosis and TCA cycle flux in rat brain during [2-^{13}C]glucose infusion. J. Neurochem. *76*, 975–989.

Stanimirovic, D.B., Ball, R., Small, D.L., and Muruganandam, A. (1999). Developmental regulation of glutamate transporters and glutamine synthetase activity in astrocyte cultures differentiated in vitro. Int. J. Dev. Neurosci. *17*, 173–184.

Tanaka, K., Watase, K., Manabe, T., Yamada, K., Watanabe, M., Takahashi, K., Iwama, H., Nishikawa, T., Ichihara, N., Kikuchi, T., et al. (1997). Epilepsy and exacerbation of brain injury in mice lacking the glutamate transporter GLT-1. Science *276*, 1699–1702.

Tong, G., and Jahr, C.E. (1994). Block of glutamate transporters potentiates postsynaptic excitation. Neuron *13*, 1195–1203.

Ullian, E.M., Sapperstein, S.K., Christopherson, K.S., and Barres, B.A. (2001). Control of synapse number by glia. Science *291*, 657–660.

Watase, K., Hashimoto, K., Kano, M., Yamada, K., Watanabe, M., Inoue, Y., Okuyama, S., Sakagawa, T., Ogawa, S., Kawashima, N., et al. (1998). Motor discoordination and increased susceptibility to cerebellar injury in GLAST mutant mice. Eur. J. Neurosci. *10*, 976–988.

Yamada, K.A., and Tang, C.M. (1993). Benzothiadiazides inhibit rapid glutamate receptor desensitization and enhance glutamatergic synaptic currents. J. Neurosci. *13*, 3904–3915.

Yamada, K., Watanabe, M., Shibata, T., Nagashima, M., Tanaka, K., and Inoue, Y. (1998). Glutamate transporter GLT-1 is transiently localized on growing axons of the mouse spinal cord before establishing astrocytic expression. J. Neurosci. *18*, 5706–5713.

Yarowsky, P., Boyne, A.F., Wierwille, R., and Brookes, N. (1986). Effect of monensin on deoxyglucose uptake in cultured astrocytes: energy metabolism is coupled to sodium entry. J. Neurosci. *6*, 859–866.